Initiation of spin-transfer torque by thermal transport from magnons

John C. Slonczewski*
Katonah Research Center, 161 Allison Road, Katonah, New York 10536, USA
(Received 24 June 2010; published 3 August 2010)

As now practiced in experimental nanomagnetic spintronics, spin-transfer torque acting on a free metallic moment is driven by electric current flowing serially through it and a metallic reference magnet. I propose driving spin-transfer torque by flow of heat serially through the free magnet and an insulating reference ferrite. The needed spin current initiates from magnons present in the ferrite. A quantum yield of heat-driven in-plane spin-transfer torque can be substantially greater, in principle, than that achievable using electric current in a magnetic tunnel junction. A Bloch-type dynamical equation for the conduction-electron-spin polarization excited by a paramagnetic-monolayer model of the ferrite/metal interface predicts the dependence of this yield on material parameters. In practice, achieving a high yield beneficial to applications will require strong exchange coupling of the local 3*d*-electron atomic spins in this monolayer to both to the ferrite moment with ferromagnetic sign and also with either sign to the conduction *s* electrons in a normal metallic spacer. Advantageous will be suppression of the interfacial heat flow diverted to phonons within the ferrite. If a nonmagnetic electrically insulating layer additionally adjoins the free magnet, the theory also predicts a perpendicular spin-transfer torque component whose angular dependence mimics conventional uniaxial magnetic anisotropy.

DOI: 10.1103/PhysRevB.82.054403 PACS number(s): 85.75.−d, 73.50.Lw, 72.25.Pn, 71.36.+c

The transfer of spin momentum driven by electric current, flowing either through a tunnel barrier[1] or metallic spacer,[2,3] is known to create pseudotorques on the macroscopic spin moments of its magnetic electrodes. Experiments in ca. 100-nm-scale multilayers[4,5] confirmed the phenomena[3] of transient switching and steady magnetic precession. Intensive investigation currently seeks to establish the usefulness of such excitations by spin-transfer torque (STT), using magnetic tunnel junctions (MTJs), in random-access memory (MRAM)[6] and nanoscopic oscillators.[7] A large yield of torque per unit driving current is vital to the success of such applications.

Other experiments already confirm the creation of STT by flow of pure spin current through a metal region well separated from the region carrying the driving electric current.[8,9] An even earlier experiment[10] used ferromagnetic resonance to confirm the creation by spin pumping[11] without any electric current, of spin-transfer torque originating from a magnetic precession. This communication proposes yet another way to create STT without electric current. It describes a *thermagnonic* process that uses flow of heat to transfer spin momentum from the thermal-magnon concentration existing within an electrically resistive ferromagnet or ferrimagnet, for brevity referred to here as a ferrite, through a normal metal into the free magnet.

A recent study demonstrated the novel spin-Seebeck effect, in which the flow of heat along an extended metallic ferromagnetic metal generates spin voltage.[12] Recent theories of this effect are based on transport of heat by motions of conduction electrons in the ferromagnetic metal.[13,14]

Significantly, Hatami *et al.*[15] had earlier predicted a substantial thermally driven STT effect in all-metallic spin valves. Indeed, experiments by Yu *et al.*[16] now report thermal influence on field-induced switching in an all-metallic spin valve.

In a different vein, a recent experiment detected an electric signal stimulated by a macroscopic spin wave within the insulating ferrimagnet $Y_3Fe_5O_{12}$ (called yttrium iron garnet).[17] This wave is excited by a radio-frequency magnetic field. A coupling of this spin wave to conduction electrons in an adjoining Pt layer creates a spin current which is detected as a spin-Hall voltage. Very recent work[18] predicts an effect in the opposite direction, showing how spin accumulation initially present in a normal metal can excite magnons in a proximate ferrimagnetic insulator by *s-d* exchange interaction.

The present communication shows how a combination of ideas in some of the cited works and others gathered in a recent special journal issue[19] can foster a highly effective thermal method of driving STT. In this method, flow of heat through a multilayer composed of very thin films carries with it spin polarization. The needed spin accumulation initiates from thermal magnons in a ferrite, instead of the usual spins transported by conduction electrons in a magnetic metal. Metallic spin current originates from super-exchange coupling between the ferrite bulk and an interfacial magnetic monolayer that is also coupled by *s-d* exchange to conduction electrons in the normal metal. The flow of spin current through this metal to a free magnet completes the conversion of spin momentum into pseudotorque.

The huge "spin accumulation" of thermal magnons polarized along the axis of spontaneous magnetization naturally present in a ferrite at nonzero temperature might be considered useless for spin transfer because magnons lack the electric charge needed to be driven by an applied electric field. However, magnons, unlike electrons, can be created and annihilated at an interface with a metal, along with the transfer of heat energy. Coulomb-exchange interactions conserve all three Cartesian components of spin density in such a process. Therefore, the creation or annihilation of magnons at an interface between a ferrite and a metal transfers magnon spin momentum into spin current within the metal, through which it may flow into a free magnet and create the desired torque.

In the treated model, a Bloch-type equation describes dynamics of noble-metal *s*-electron spins coupled to an assumed paramagnetic monolayer lying at the crucial ferrite/

metal interface. Its solution describes the spin current which accompanies heat flow between the ferrite and the metal. The result predicts how the strength of thermagnonic transfer of the in-plane component of spin depends on exchange interactions coupling these interfacial spins to both the ferrite moment and the conduction electrons within the metallic spacer. Achieving a significant increase in STT yield over what is available from MTJs also requires suppression of the competitive interfacial heat flow between ferrite phonons and metal electrons.

Estimates based on measured properties of selected spinel ferrites show that the thermagnonic mechanism should yield a greater in-plane torque with electric current flowing through a heating resistor than the torque available using an equal electric current flowing through a magnetic tunnel junction.

The creation of an additional, plane perpendicular, component of thermagnonic STT requires the presence of an optional nonmagnetic electric insulator lying on the side of the free magnet opposite to that of the ferrite. This insulator may be a tunnel barrier such as one often used in spintronic devices. This component of torque mimics that derivable from a uniaxial magnetic anisotropy of the free magnet; its symmetry axis lies parallel to the ferrite moment.

This paper is sectioned in the following sequence: description of the proposed multilayer structure, heuristic argument for expecting a very strong thermagnonic quantum torque yield, description of the Bloch-equation basis of the subsequent analysis, derivation of the intrinsic in-plane component of torque yield, account of the competitive effect of heat transport by phonons, estimates of useful torque yield and temperature differential based on experimental data for spinel ferrites and noble metals, derivation of the plane-perpendicular component of thermagnonic torque, summary and discussion.

I. MULTILAYER STRUCTURE

Figure 1(a) shows one possible arrangement of the components required for thermagnonic spin transfer in a multilayer. Beginning at the left, a steady source provides heat flow Q rightward sequentially through a ferrite film having a uniform pinned (if necessary) static spin moment $\hbar\mathbf{S}_{\mathrm{frt}}$ per unit area, a normal-metal film, a metallic free magnet with spin moment $\hbar\mathbf{S}_{\mathrm{fm}}$ per unit area that is excitable via the classical Landau-Lifshitz equation, and finally into a thermal bath consisting of another metal or other nonmagnetic material with sufficient thermal conduction to disperse the incoming heat without significant rise of temperature. As indicated, an optional thin electric insulator may lie between the free magnet and the thermal bath.

In a nanoscopic thermagnonic device, such as a spin-transfer oscillator or a memory cell, an electric current may supply the needed Joule heating. The tunneling barrier used in thermally assisted MRAM provides an example of such a heater.[20] [If it were used here, the direction of heat would naturally oppose that shown in Fig. 1(a).] Use of such a tunnel barrier to provide the heat would require circuit closure by flow of electricity through the spacer in some direction parallel to the film plane. However, since electric current plays no part in the physics of thermagnonic spin transfer, one may better imagine that the incident beam of light indicated in Fig. 1(a) provides the heat.

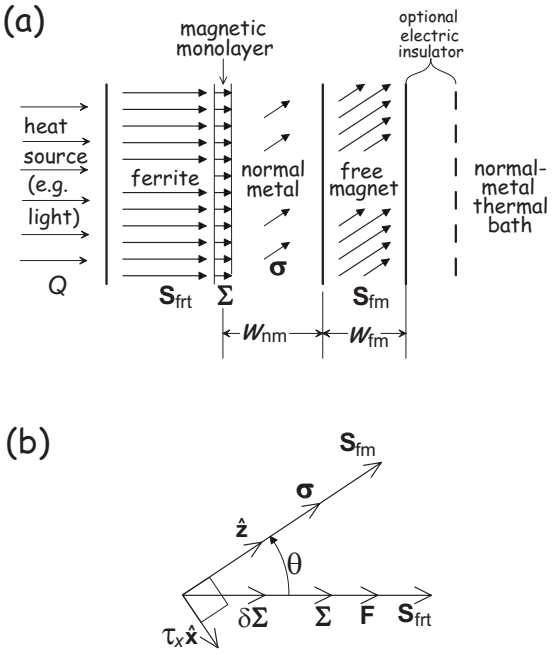

FIG. 1. (a) Schematic arrangement of the elements required for creating in-plane torque on a free magnet by thermally initiating spin transfer from magnons present in a nonmetallic reference magnet. Out-of-plane torque is negligible unless the indicated optional insulator (e.g., tunnel barrier) is present in the multilayer. (b) Geometric relationships and notations for the in-plane torque component $\hbar\tau_x\hat{\mathbf{x}}$ and the spin moments indicated in panel a, together with the time-dependent Cartesian unit vectors $\hat{\mathbf{x}}$ and $\hat{\mathbf{z}}$. (The unit vector $\hat{\mathbf{y}}=\hat{\mathbf{z}}\times\hat{\mathbf{x}}$ and the out-of plane torque component $\tau_y\hat{\mathbf{y}}$ are not shown.)

II. HEURISTIC QUANTUM YIELD

Any integrated circuit transistor has a practical limit, sometimes considered to be 1 μA per nm of gate width, on the electric current it can supply.[6] In application to STT-MRAM, this limit places great importance on the STT per unit current needed to switch a free magnet. In this case of current-driven STT, one may usefully define a numerical quantum yield ε of STT by the ratio

$$\varepsilon = \left| \frac{\text{transferred spin momentum}}{\hbar} \Big/ \frac{\text{spent electric charge}}{e} \right| \tag{1}$$

when the pinned and free moments are orthogonal. Consider the example of an MTJ using half-metallic ferromagnets. Suppose that one electron, carrying charge e, tunnels through the barrier. By this definition, it transfers spin momentum $\hbar/2$ resulting in the quantum yield $\varepsilon_{\mathrm{mtj}}=1/2$, independently of the voltage across the barrier. Experiments with MgO barriers approach $\varepsilon_{\mathrm{mtj}}=1/2$,[21,22] a value that cannot be exceeded using a single barrier.

A comparable definition of quantum yield (now voltage dependent) may serve for thermagnonic spin transfer in the scheme of Fig. 1(a) if we imagine some unspecified heating device that creates the heat flow $Q=IV$. Suppose STT originates by flow of heat initiated by magnons following thermalization of the energy provided by one electron falling through the potential V applied across the heater. If this heater is an ordinary resistor, incandescent light, or tunnel barrier, then V is obviously the voltage across this resistive element. If the heat source is light created by a light-emitting diode or semiconductor laser, then V is the band gap of the electronic transition. (This definition of ε is not of universal usefulness; it makes little sense in case one drove STT with the spin current generated by applying rf excitation to YIG.[17])

We will make the following heuristic estimate of ε for the thermagnonic case: each magnon has typical energy of the order k_BT, where $T=300$ K is the ambient temperature and carries a spin component $\hbar s_\zeta=-\hbar$ where the ζ axis is along $\mathbf{S}_{\rm frt}$. If the spin of each magnon that is annihilated at the ferrite/metal interface is ultimately transported to the free magnet, the heuristic yield from Eq. (1) is the average number of magnons per spent electron, or of the order

$$\varepsilon_{\rm htc} \approx eV/k_BT = 40 \text{ per applied volt}. \quad (2)$$

A more cautious approach to $\varepsilon_{\rm htc}$ is from leading terms of standard low-temperature expansions of magnon number density $n(T)$ and magnetic specific heat $C(T)$.[23] Thus one evaluates the yield $\varepsilon_{\rm htc}=(dn/dT)C^{-1}eV$ to be, after substitution of Walker's expansions, $\varepsilon_{\rm htc}=30.1$ per volt at $T=300$ K, which differs little from Eq. (2). These considerations suggest the possibility of a significant improvement of spin-transfer torque by driving it with heat instead of electricity that is only capable of $\varepsilon_{\rm mtj}\leq 1/2$ in MTJs.

III. BLOCH EQUATION

Crucial to realistic estimation of thermagnonic spin transfer is the microscopic mechanism for transfer of spin current between the magnon carriers in the ferrite and the conduction-electron carriers in the normal-metal spacer. [See Fig. 1(a).] As mentioned above, the experiment of Kajiwara *et al.*[17] provides evidence of coupling to conduction electrons in the case of macroscopic spin waves. In our model of this mechanism, we assume the presence of an interfacial atomic monolayer containing local paramagnetic $3d$-electron-spin moments that are exchange coupled to both the ferrite moment and the conduction electrons in the metal. A later section of this communication specifies a spacer composed of a noble metal (Cu, Ag, or Au) and a monolayer containing Mn or Fe nuclei. These two exchange effects provide the means of transporting heat and spin momentum between ferrite magnons and metal electrons for ultimate transfer of spin momentum as pseudotorque into the adjoining free magnet. This monolayer might arise naturally during the multilayer deposition or be deposited specially.

This paramagnetic monolayer has $N_{\rm d}$ magnetic ions or atoms per unit area, each with spin operator $\hbar\mathbf{S}_j (j=1,2,\ldots,N_{\rm d})$, spin quantum number S, and Landé factor $g=2$. Its thermal average spin moment per unit area is $\boldsymbol{\Sigma}=\langle\Sigma_j\mathbf{S}_j\rangle$. An effective exchange energy $-\mathbf{F}(T)\cdot\mathbf{S}_j$ couples each spin to the moment $\mathbf{S}_{\rm frt}$ of the ferrite by superexchange.[24] The splitting field magnitude F is usually smaller than the molecular field occurring within the bulk of the ferrite because the number of relevant $3d$-O^{2-}-$3d$ exchange routes is smaller. At thermal equilibrium, with $\Sigma=\Sigma_0$, the polarization is $\Sigma_0\equiv\chi_{\rm d}F$ where, according to the Curie law

$$\chi_{\rm d} = S(S+1)N_{\rm d}/3k_BT. \quad (3)$$

The deviation, due to steady heat flow, of monolayer moment from thermal equilibrium is written

$$\boldsymbol{\delta\Sigma} = (\Sigma - \chi_{\rm d}F)(\hat{\mathbf{x}}\sin\theta + \hat{\mathbf{z}}\cos\theta) \quad (0<\theta<\pi). \quad (4)$$

[See Fig. 1(b).] Here the static field $\mathbf{F}(T)$ has the direction $\pm\mathbf{S}_{\rm frt}$, where the sign depends on the signs and magnitudes of the exchange coefficients that couple $\mathbf{S}_j$ to one, two or three magnetic sublattices in the ferrite. Here, θ is the angle between $\mathbf{F}$ and the generally dynamic spin moment $\mathbf{S}_{\rm fm}=S_{\rm fm}\hat{\mathbf{z}}(t)$ of the free magnet; $\hat{\mathbf{x}}(t)$, $\hat{\mathbf{y}}(t)$, and $\hat{\mathbf{z}}(t)$ are orthogonal unit vectors in three-dimensional space.

To treat the thermal transport of heat and spin across this crucial interface, we adapt (with modified notation) a Bloch-type equation derived for an unbounded dilute magnetic alloy such as Cu:Mn.[25–27] The following Hamiltonian, which includes no interactions other than Coulomb exchange, governs a unit volume of such a dilute paramagnet in which, for our purpose, the field $\mathbf{F}$ would act on $\mathbf{S}_j$ (located at random in three dimensions) but not on the conduction-electron spins $\mathbf{s}_i$:

$$H = \sum_{i=1}^{n}(\mathbf{p}_i^2/2m_e) - \mathbf{F}\cdot\sum_{j=1}^{N}\mathbf{S}_j - (J_{\rm sd}/n)\sum_{i,j}\mathbf{s}_i\cdot\mathbf{S}_j. \quad (5)$$

Here m_e is electron mass, $\mathbf{p}_i$ is the momentum operator of a free electron, $J_{\rm sd}$ is the on-site sd exchange coupling, N is the number of local $3d$-electron magnetic sites and n ($\gg N$ for dilution) is the number of s electrons. Our model assumes that the Bloch equation derived for such a statistically homogeneous system also holds for our structured system in which magnetic atoms occupy interfacial monolayer sites.

Write the average thermal s-electron-spin moment for unit film area $\boldsymbol{\sigma}=\langle\Sigma_i^{N_{\rm s}}\mathbf{s}_i\rangle$. Here $N_{\rm s}$ is the number of conduction s electrons (considered free, one per atom) within the metal spacer including the paramagnetic monolayer. Its time derivative is denoted $\dot{\boldsymbol{\sigma}}\equiv d\boldsymbol{\sigma}/dt$. The Bloch-type dynamic equation[28] for $\boldsymbol{\sigma}$ due to its interaction with $\boldsymbol{\Sigma}$ is rewritten and simplified in the form

$$\dot{\boldsymbol{\sigma}} + \lambda\boldsymbol{\Sigma}\times\boldsymbol{\sigma} = \nu_{\rm ds}\boldsymbol{\delta\Sigma} - \nu_{\rm s}\boldsymbol{\sigma}. \quad (6)$$

(An additional interaction of $\boldsymbol{\sigma}$ with $\mathbf{S}_{\rm fm}$ will be taken into account below.) Here, the d-to-s spin-relaxation rate[29] is

$$\nu_{\rm ds} = (\pi/\hbar)(J_{\rm sd}\rho)^2k_BT, \quad (7)$$

where ρ is the density of s-electron states per atom, for each spin direction, present in the paramagnetic monolayer and the noble-metal spacer. In Eq. (6), the coefficients λ and $\nu_{\rm s}$ are adjustable. The coefficient λ governs the precession of

the s-electron moment $\boldsymbol{\sigma}$ caused by exchange-coupled scattering of s electrons by the d-electron monolayer moment $\boldsymbol{\Sigma}$; ν_s governs the sum of s-to-d, s-to-lattice, and longitudinal s-to-free-magnet spin relaxations. Evaluation of λ and ν_s would involve exchange and spin-orbit couplings, and electron-structure parameters of the free magnet; thus it lies outside of the scope of this communication.

Our model assumption above of an sd interaction coupling the ferrite to the normal metal was already made in the work of Takahashi *et al.*[18] cited above. This assumption differs from that in the very recent work of Xiao *et al.*[30] who assumed such a coupling by the effect of spin pumping.

The right-hand side of Eq. (6), with the formula (7), follows from lowest-order "golden-rule" transition-rate theory. Our simplification of the Bloch equation neglects sd hybridization and stationary effects of virtual sd-exchange excitation of the electron gas.[27] In our model system, such neglected effects give rise to: (i) a static induced polarization of the s electrons and effective RKKY exchange coupling between different $\mathbf{S}_j$ amounting to an adjustment of $\mathbf{F}$. For example, *ab initio* computations for magnetic adatoms on a *free* surface of Cu(111) predict oscillatory interadatomic exchange couplings versus separation for Cr amounting to as much as 10 meV at the first maximum.[31] (If these correlations are positive, their inclusion would probably tend to increase the strength of STT predicted below.); (ii) a static spatially oscillatory RKKY-type exchange interaction energy between $\boldsymbol{\Sigma}$ and $\mathbf{S}_{\mathrm{fm}}$, which is proportional to the expression $w_{\mathrm{nm}}^{-2}\cos(kw_{\mathrm{nm}}+\phi)$ where k satisfies a "caliper" condition within the Fermi surface of the normal-metal spacer,[32] and w_{nm} is its thickness; and (iii) Kondo effect or giant-moment corrections significant at low temperature.[27]

Although one may object to reliance on linear susceptibility in the presence of possibly large F (considered below), application of Eq. (6) should provide a reasonable estimate of thermagnonic STT caused by flow of heat. This torque should be added to other torque terms well known in the phenomenological Landau-Lifshitz equation governing the dynamics of the free magnet.

IV. IN-PLANE TORQUE

The conditions $\boldsymbol{\sigma}=0$ and $\boldsymbol{\delta\Sigma}=0$ hold in static thermal equilibrium, the latter according to definitions (4) and (3). Suppose the temperature of the ferrite spins including the monolayer moment differs from that of the adjoining metal. Then $\boldsymbol{\Sigma}$ deviates from $\boldsymbol{\Sigma}_0$ by a first-order amount $\boldsymbol{\delta\Sigma}$. Our problem is to solve Eq. (6) for $\boldsymbol{\sigma}$ and $\dot{\boldsymbol{\sigma}}$.

Prior to solving this equation, we should account qualitatively for the effect on $\boldsymbol{\sigma}$ and $\dot{\boldsymbol{\sigma}}$ of exchange interaction with the free magnet. Consider an intermediate time scale for $\boldsymbol{\sigma}(t)$ lying between the 10^{-11} to 10^{-10} s. scale of free-moment dynamics governed by the Landau-Lifshitz equation and the $w_{\mathrm{nm}}/v_{\mathrm{F}}\approx 10^{-14}$ s scale of assumed back-and-forth ballistic s-electron scattering at the interfaces of a $w_{\mathrm{nm}}\approx 5$ nm-thick normal-metal spacer. On this intermediate time scale ($\approx 3\times 10^{-13}$ s), the strong s-d exchange (≈ 0.5 eV) within the free magnet causes its moment $\mathbf{S}_{\mathrm{fm}}=S_{\mathrm{fm}}\hat{\mathbf{z}}$ to rapidly absorb transverse (x and y) components of $\boldsymbol{s}_i$, creating a torque $\hbar\boldsymbol{\tau}$ per unit film area. It follows that σ remains approximately collinear with $\mathbf{S}_{\mathrm{fm}}$. [See Fig. 1(b).]

In case the optional insulating film shown in Fig. 1(a) is present, it blocks escape of electrons beyond the free magnet into the thermal bath, thus ensuring the complete absorption of $\dot{\sigma}_x$ and $\dot{\sigma}_y$ by the free magnet.[33] (According to the latter reference, torque arises even if the free magnet is insulating.) However, if no insulator other than the ferrite polarizer is present, heated electrons may carry spin into the thermal bath. Then the nearly complete absorption by the free magnet nevertheless still follows as shown by effective-potential[34] and *ab initio*[35] calculations.

These considerations justify the approximate simplification of Eq. (6) with the substitutions

$$\boldsymbol{\sigma}=\sigma\hat{\mathbf{z}},\quad \dot{\boldsymbol{\sigma}}=\boldsymbol{\tau}\equiv\tau_x\hat{\mathbf{x}}+\tau_y\hat{\mathbf{y}}. \tag{8}$$

The component $\hbar\tau_x$, known in the literature for current-driven spin transfer as in-plane torque, follows directly from the x component of Eq. (6) with substitution of the Eqs. (4) and (8):

$$\tau_x=\nu_{\mathrm{ds}}\delta\Sigma\,\sin\theta\equiv\tau_{x0}\sin\theta.\quad(0<\theta<\pi) \tag{9}$$

We term the yield $\varepsilon_{\mathrm{int}}$ of thermagnonic spin transfer defined by Eq. (1) as *inherent* when disregarding thermal transport by phonons (considered below). First consider the energy $E_{\mathrm{d}}=-\mathbf{F}\cdot\boldsymbol{\Sigma}$ of the local interfacial spin moment in the molecular field $\mathbf{F}$ of the ferrite. The heat flux taken from the local spin monolayer to the normal metal for $\theta=\pi/2$ has the alternative expressions

$$Q_{\mathrm{ds}}\equiv -dE_{\mathrm{d}}/dt=F\dot{\Sigma}=-F\tau_{x0}=-F\nu_{\mathrm{ds}}\delta\Sigma, \tag{10}$$

where the third equality comes from Coulomb-exchange conservation of spin ($\dot{\Sigma}_x+\dot{\sigma}_x=0$) and Eq. (8); the last equality from Eq. (9).

Imagine a spintronic device which somehow generates the interfacial heat flux by Joule heating with $Q_{\mathrm{ds}}=IV$. Then our inherent quantum yield by definition (1) and the third equality of Eq. (10) is

$$\varepsilon_{\mathrm{int}}=\left|\tau_{x0}\frac{e}{I}\right|=|eV/F|. \tag{11}$$

In place of $k_{\mathrm{B}}T$ in Eq. (2) we now have the exchange energy F, which may be smaller, transferred during the transfer of each spin unit.

V. USEFUL QUANTUM YIELD

A. Interfacial heat conductance

Accounting for the competition for heat flow between spin couplings and lattice vibrations will correct the incredible inverse dependence of $\varepsilon_{\mathrm{int}}$ on F in the latter equation. The bulk thermal phonon resistance in a sufficiently thin insulator is negligible in comparison with the interfacial resistance.

Theoretically, the thermal conductance G_{Kap} across a normal insulator-metal interface, known as Kapitza conductance, may be dominated at $T=300$ K by interfacial scatter-

ing of phonons[36] or by coupling of insulator phonons to the electron gas in the metal as proposed by Mahan.[37] In our system, the mean-free-electron path (31 nm in Cu, 58 nm in Ag, and 42 mn in Au) is dominated by scattering from phonons. Consider the normal-metal film thickness to be much smaller than this. Then Mahan's mechanism is likely more relevant here because the thermal electrons in the conduction-electron gas excited by interaction with magnons have little internal contact with the metal phonons.

Let us assume that heat flow carried by spins is also dominated by interfacial spin conductance G_{fs} from ferrite to *s*-electron gas in the spacer. Then the torque yield [Eq. (11)] is reduced simply by the proportion $G_{fs}/(G_{Kap}+G_{fs})$ of heat carried across the interface by exchange to the total. Thus we modify Eq. (11) by writing for the *useful* yield

$$\varepsilon_{us} = |eV/F|[1 + (G_{Kap}/G_{fs})]^{-1}, \quad G_{fs} = (G_{fd}^{-1} + G_{ds}^{-1})^{-1}, \tag{12}$$

where the exchange resistance G_{fs}^{-1} has two additive terms: G_{fd}^{-1} for ferrite to *d* monolayer, and G_{ds}^{-1} for *d* monolayer to *s* metal.

A note of caution: The heat source, such as the light in Fig. 1(a), may preferentially favor the magnon or phonon baths. Then the latter equation may overestimate or underestimate ε_{us}. If this is the case, insertion of a normal-metal layer between the heat source and the ferrite will favor Eq. (12) on the assumption that Mahan's[37] phonon/conduction-electron mechanism for G_{Kap} dominates.

B. Monolayer-to-metal heat conductance

To obtain the yield, we need to estimate the two exchange-mediated conductances appearing in Eq. (12). To estimate the coefficient G_{ds}, whose inverse turns out to be dominant, note that $\delta\Sigma$ relates to temperature according to $\delta\Sigma = (d\chi_d/dT)F\delta T_{ds}$, where $\delta T_{ds} = (T_d - T_s)$ is the first-order temperature difference between the interfacial layer and the normal metal. (Our neglect of the dependence of F on T modestly underestimates the magnitude of $\delta\Sigma$ and therefore ε_{us} in the following argument.) The result from Eq. (3) is

$$\delta\Sigma = -F\chi_d\delta T_{ds}/T. \tag{13}$$

By substituting this equation and Eq. (7) into the last expression in Eq. (10) and using Eq. (3), we find, independently of θ,

$$G_{ds} = Q_{ds}/\delta T_{ds} = \pi S(S+1)N_d[\rho J_{sd}F(T)]^2/3\hbar T. \tag{14}$$

C. Ferrite-to-monolayer conductance

Although usually smaller than G_{ds}^{-1}, the ferrite-to-monolayer resistance G_{fd}^{-1} may contribute significantly to yield given by Eq. (12) if F is small. A magnon with wave-vector $\mathbf{k}$ and energy $\varepsilon(\mathbf{k})(>0)$ carries the spin component $s_\zeta(\mathbf{k}) = -1$ along the spin-moment axis ζ. Considering occupation numbers $n(\mathbf{k},T)$, the ferrite polarization, in $\hbar$ units, is $S_{frt,\zeta}(T) = S_{frt}(0) - \Sigma_{\mathbf{k}}n(\mathbf{k},T)$; its internal energy is $E_{frt} = \Sigma_{\mathbf{k}}\varepsilon(\mathbf{k})n(\mathbf{k},T)$.

Any single-magnon creation or annihilation $\Delta n(\mathbf{k},T) = \pm 1$ at the interface must obey conservation of energy and spin. Consider the relation $E_d = -F\Sigma_j S_{j.\zeta} = -F\Sigma_j m_j$ in which the integer m_j satisfies $-S \le m_j \le S$. Energy conservation gives $\Delta n(\mathbf{k})\varepsilon(\mathbf{k}) - F\boldsymbol{\Delta}m_j = 0$ for some j and conservation of spin gives $-\Delta n(\mathbf{k}) + \boldsymbol{\Delta}m_j = 0$. Combining these two relations gives $\varepsilon(\mathbf{k}) = F$, which implies that the associated conductance G_{fs} in this model vanishes unless the ferrite-monolayer coupling is ferromagnetic ($F > 0$).

Because the thermal resistance G_{fd}^{-1} proves to have little effect on the quantum yield, we omit many details in its derivation. We use a semiclassical treatment of thermal-magnon excitation of the monolayer spins following the textbook derivation for absorption of light by an atom.[38] One replaces the dipole interaction of the light wave with the perturbation defined by $-\mathbf{F}\cdot\mathbf{S}_j = -FS_{j,\zeta} + H_{pert}$ that couples the small-amplitude classically precessing spin-wave magnetization field (with wave-vector k) to the jth monolayer spin:

$$H_{pert} = -F\beta(T)(S_{j,\xi}\cos\omega\tau + S_{j,\eta}\sin\omega t). \tag{15}$$

Here ξ, η, ζ are fixed Cartesian axes, $\beta(T)(\ll 1)$ is the cone angle for ferrite spin-wave precession at the frequency $\omega = \alpha_{es}k^2$ where α_{es} is a continuum exchange stiffness coefficient.[23] Resonant energy exchange occurs for $\hbar\omega = F$ under the ferromagnetic-coupling condition $F > 0$ derived above. Using Maxwell statistics for the spin waves, one finds for the semiclassical ferrite-to-monolayer heat rate per unit area

$$Q_{fd} = S(S+1)(e/m_e)F^{7/2}/3\pi\alpha_{es}^{3/2}M(0)T, \tag{16}$$

where $M(T)$ is the magnetization per unit volume of the ferrite.

One may apply Walker's expression[23] for the low-temperature $T^{3/2}$ law of magnetization

$$[M(0) - M(T)] = KT^{3/2}, \tag{17}$$

where

$$K = 0.653\mu_\beta(k_B/\pi\alpha_{es})^{3/2} \tag{18}$$

and μ_β is the Bohr magneton. Elimination of K and α_{es} between the latter three equations results in

$$G_{fd} = \frac{dQ_{fd}}{dT} = \frac{1.81S(S+1)N_dF^{7/2}\delta m(T)}{\hbar k_B^{3/2}T^{5/2}}, \tag{19}$$

where

$$\delta m(T) \equiv [M(0) - M(T)]/M(0). \tag{20}$$

Thus the form of Eq. (19) enables estimation G_{fd} by recourse to only one additional parameter $\delta m(T)$ obtainable from experimental data for $M(T)$ of the ferrite.

VI. ESTIMATES

Lack of information about G_{Kap} for ferrite/metal interfaces at T near 300 K makes estimation of the Kapitza effect

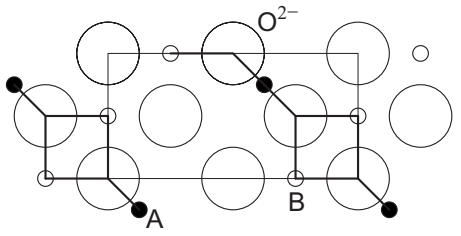

FIG. 2. Projected crystalline structure of a spinel monolayer interface assumed to adjoin a noble metal (atoms not shown). 100 texture of the spinel film is assumed. In a spinel crystal $(A)[B_2]O_4$, O^{2-} sites form a nearly perfect fcc lattice whose lattice parameter is half that (a) of the spinel. In the interface structure, B and O^{2-} sites are coplanar but A sites lie on a plane $a/8$ distant on the ferrite side of the plane containing B and O^{2-} sites.

on ε_{us} uncertain. However, we note that data for one set of 11 reported nonmagnetic compositions[36] include the values $G_{Kap}=(40,45,40)$ MW/m^2 K for (BaF_2, Al_2O_3, and diamond), respectively, each interfacing Au. Since these values depend weakly on the composition of the insulator, we might assume a similar value for the interface between a ferrite and Au. Moreover, if this is correct, Kapitza resistance dominates over measured bulk resistances of commercial ferrites less than 200 nm in thickness. However, examples of higher G_{Kap} exist, such as 112 MW/m^2 K for sapphire/Ti.[36] Let us assume that interfaces also dominate heat conduction via spin-exchange interactions. Then, for such thin ferrite films, we may use the purely interfacial Eq. (12) with substitutions from Eqs. (14) and (19) to estimate the thermagnonic STT yield.

Experimental data for heat capacity of the noble metals[39] provide values of state density ρ. Magnetic susceptibilities versus T for the respective highly dilute magnetic alloys Cu:Mn, Ag:Mn, and Au:Mn as measured[40] and interpreted[41] provide values of J_{sd} for the spin state $S=5/2$ of the $3d^5s$ electron configuration of a Mn substitution. Since these measured values depend little on the atomic number of the solvent, we take $\rho=0.15$ eV^{-1} spin^{-1} atom^{-1} and $J_{sd}=-0.5$ eV to represent any one of these three alloys. For values of N_d and F, we consider two models of atomic structure of the ferrite/spacer interface which assume one of two possible crystalline textures of the deposited ferrite film.

A. 100 texture

For the case of 100 texture, the metallic spacer is assumed to bind chemically to an unreconstructed 100 plane of the cubic spinel-ferrite $(A)[B_2]O_4$ structure[42] which contains B sites and O^{2-} sites but no A sites. Figure 2 shows a projection of the structure of this plane, in which the rectangle indicates one cell of the two-dimensional periodic lattice. Its dimensions are indicated in terms of the spinel lattice parameter a. It also shows a projection of the A sites lying within the first neighboring atomic plane distant $a/8$ on the spinel side of the B interface. Heavy lines in the figure indicate routes of the dominant superexchange coupling between A and B sites. In the spinel, O^{2-} ions lie on a cubic, nearly fcc Bravais lattice with lattice

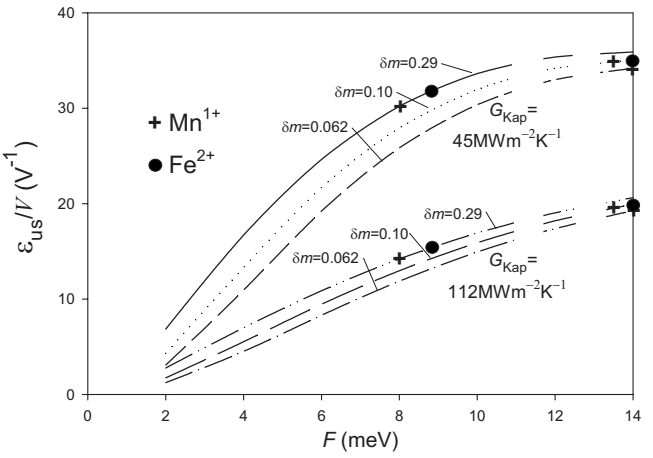

FIG. 3. Predicted useful thermagnonic spin-transfer yield, per volt (with $V>0$) that is applied to an imagined Joule heater, versus exchange splitting energy F acting on the magnetic monolayerinterface. The corresponding yield for an MTJ is $\varepsilon_{mtj}\leq 1/2$, independent of voltage. Two possible values of interfacial thermal conductivity G_{Kap} are considered. The dimensionless coefficient $\delta m=(0.062,0.10,0.29)$ of experimental magnetization decrement at $T=300$ K corresponds to the spinel-ferrite compositions Fe_3O_4, $(Fe)[NiFe]O_4$, $(Mn)[Fe_2]O_4$, respectively (Ref. 43). The assumed density $N_d=5.7\times10^{18}$ m^{-2} of magnetic sites with $S=5/2$ on the interface is appropriate to the assumed interfacial structure shown in Fig. 2 for 100 ferrite-film texture. The plots show points (+ and ●) of F for local moments Mn^{1+} and Fe^{2+}, shown in Table I, as estimated from tabulated properties of ferrites (Ref. 43), adjusted for atomic charge.

parameter $a/2$. Magnetic atoms or ions lying on the B sites shown constitute the magnetic monolayer of the theory with density $N_d=N_{100}\equiv 4/a^2=5.7\times10^{18}$ m^{-2} for spinel ferrites generally. No special interfacial order or disorder is required for the crystalline noble metal (whose atoms are not shown in Fig. 2) abutting the ferrite. However, the noble metal should be metallically bound to the A and B sites, and ionically bound to the O^{2-} sites shown in Fig. 2. Our ballistic treatment of electron transport in the spacer requires its noninterfacial bulk to be crystalline.

First consider the superexchange splitting F of an interfacial magnetic site to be adjustable. Figure 3 shows plots of useful quantum yield per volt (applied to an imagined Joule heater) *versus* F predicted by Eqs. (12), (14), and (19) and the parameter values given above. The assumed temperature is $T=300$ K. An experimental value of $\delta m(T)$, as defined by Eq. (20), characterizes the ferrite. The plotted curves assume the values $\delta m(300\ \text{K})=0.062$, 0.10, and 0.29, obtained from tabulated measurements of $M(T)$,[43] for the ferrites Fe_3O_4, $(Fe)[NiFe]O_4$, $(Mn)[Fe_2]O_4$, respectively. The inclusion of Fe_3O_4 (magnetite) in this calculation implies neglect of heat flow carried by movement of conduction electrons across the interface since magnetite is in fact an electric conductor. Breaks in the upper ranges of these curves draw attention to the limitation $F\ll k_BT$ in our reliance on the Curie law, which amounts to $F\ll 26$ meV at $T=300$ K.

Now consider what values of F are expected from known experimental properties of certain ferrite compositions. The AB exchange interactions and the spin polarity of B sites

TABLE I. Values of the B-site monolayer exchange splitting F_B at $T=300$ K expected from data for spinel ferrites. Figure 2 shows the projected interface structure assumed for this case of 100 ferrite-film texture.

Ferrite	Fe_3O_4	$(Fe)[NiFe]O_4$	$(Mn)[Fe_2]O_4$
m (300 K)	0.94	0.90	0.71
$F_{Mn^{1+}}$ (meV)	14	13.5	8.0
$F_{Fe^{2+}}$ (meV)	19	14	8.7

predominate in determining the net spin polarization of a spinel ferrite. Therefore, according to the above theory, we may neglect the magnetic heat flow through interfacial A sites because they are antiferromagnetically coupled to the net polarization. For simplicity, the generally smaller BB exchange interactions are neglected. We limit consideration of interfacial magnetic ions to those with electron structure $3d^5ns^1$ for which the vanishing orbital momentum quantum number $L=0$ insures a minimal degree of spin-lattice relaxation that tends to weaken spin-transfer torque. Also, the presence of just one s electron justifies adoption of the value $J_{sd}=-0.5$ eV because it was inferred from measurements of alloys in which the solvent noble metal contains one s conduction electron per atom.

A formula, here devised for the exchange splitting F_B of a local interfacial B moment arising from coupling to A moments, distinguishes between bulk and interfacial A and B moments. This formula

$$F_B(\text{meV}) = [0.116m(T)][H_{BA}(\text{T})/6](1+2A)B \qquad (21)$$

has four factors. The first factor, with $m(T) \equiv 1-\delta m(T) = M(T)/M(0)$, corrects for finite temperature and converts Tesla units into milli-electron volt. The second factor divides the tabulated[43] exchange field H_{BA} of A moments on a B moment in the bulk spinel by 6 to give the field due to a single A moment at $T=0$ K. The third factor sums the numbers of internal and interfacial A sites that act on the interfacial B, with the interfacial term corrected with the reduction factor A for the diminished electric charge on an interfacial A present in a neighboring parallel plane as projected in Fig. 2. The last factor B corrects for the diminished charge on the interfacial B under consideration.

The reduction factors A and B are applied whenever a cation with electronic state $3d^5$ and $S=5/2$ in bulk spinel acquires the state $3d^5ns^1$ if present in the assumed borderline condition, partially metallic and partially ionic, of the interfacial monolayer. The reductions in particular interest are $Fe^{3+} \rightarrow Fe^{2+}$ and $Mn^{2+} \rightarrow Mn^{1+}$. Data tabulated by Dionne[43] suggest the values $A \approx B \approx 0.8$, reducing Eq. (21) to F_B (meV) $\approx 0.040m(T)H_{BA}$(T). Tabulated data[43] indicate $H_{Fe,Fe}=510$ T, $H_{Mn,Fe} \approx 380$ T, and $H_{Mn,Mn} \approx 250$ T. Table I shows the expected values for superexchange splitting F_B of Mn^{1+} and Fe^{2+} placed at the assumed interfacial B sites indicated in Fig. 2, as calculated from the latter formula. Plotted points in Fig. 3 indicate values of $F_{Mn^{1+}}$ and $F_{Fe^{2+}}$ from this table that lie in the plotted range $F \leq 14$ meV.

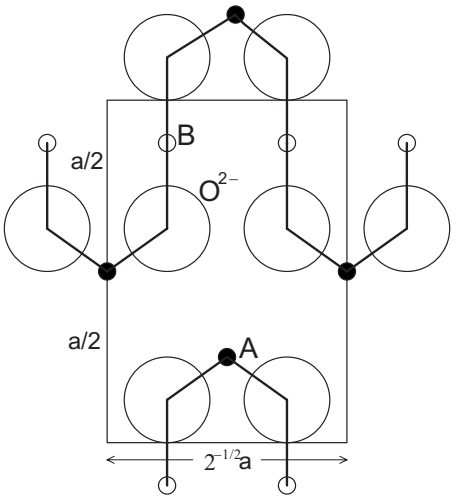

FIG. 4. As in Fig. 2, crystalline structure of a spinel monolayer interface assumed to adjoin a noble metal (not shown). Here, 110 texture of the spinel (lattice parameter a) film is assumed. The A, B, and O^{2-} sites shown are coplanar.

B. 110 texture

Figure 4 shows a 110 plane of the spinel structure which contains A, B, and O^{2-} sites. The rectangle indicates one cell of two-dimensional periodicity whose dimensions are given in terms of the spinel lattice parameter a. Since two interfacial B sites are present within each two-dimensional cell outlined by the rectangle in Fig. 2, their density is near $N_d=2^{3/2}a^{-2}=4.0\times10^{18}$ m^{-2} for spinel ferrites generally. Figure 5 shows the calculated quantum torque yield per volt for the 110 case with the same parameter values, other than N_d, as in the 100 case. The yields are now a little smaller simply because of the reduced density N_d of the monolayer magnet.

The heavy lines in Fig. 4 indicate routes of AB superexchange in the assumed interfacial structure for the case of

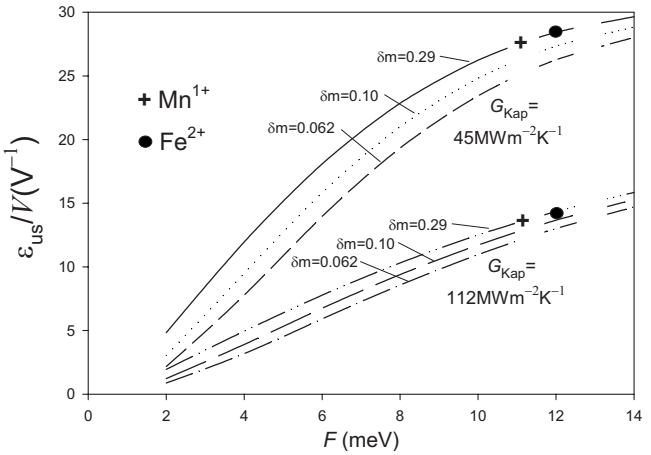

FIG. 5. Like Fig. 3 but for 110 spinel-ferrite texture. The assumed density $N_d=4.0\times10^{18}$ m^{-2} is appropriate for the assumed interfacial structure shown in Fig. 4. The plots show points (+ and ●) of F for local moments Mn^{1+} and Fe^{2+}(shown in Table II) estimated as for Fig. 3.

TABLE II. Values of the B-site monolayer exchange splitting F_B 300 K expected in certain ferrite films with assumed 110 texture, as inferred from data for bulk spinel ferrites. Figure 4 shows the interface structure assumed.

Ferrite	Fe_3O_4	(Fe)[NiFe]O_4	(Mn)[Fe_2]O_4
m (300 K)	0.94	0.90	0.71
$F_{Mn^{1+}}$ (meV)	20	19	11
$F_{Fe^{2+}}$ (meV)	27	26	12

110 texture. The A, B, and O^{2-} sites shown are coplanar. If the indicated plane lies at the ferrite-metal interface, one replaces Eq. (21) with

$$F_B(\text{meV}) = 0.116m(T)[H_{B,A}(\text{T})/6](2+2A)B \tag{22}$$

because now each interfacial B site is exchange coupled to two internal spinel A sites (not shown in Fig. 4) and the two interfacial A sites, with factor A correction for charge reduction, seen in Fig. 4. Table II shows the expected values for molecular-field splitting F of Mn^{1+} and Fe^{2+} placed at the assumed interfacial B sites indicated in Fig. 4.

VII. TEMPERATURE DIFFERENTIAL

We estimate the maximum temperature differential $\delta T = Q_{ds}/G_{ds}$ across one interface during a switch of the free magnet, neglecting the smaller of the two resistance terms G_{fd}^{-1}. G_{ds} depends negligibly on θ. For convenience, δT is expressed in terms of the torque amplitude $\hbar|\tau_{x0}|$ needed for the application. Substituting Eqs. (10) and (14) into $\delta T = Q_{ds}/G_{ds}$, we find

$$|\delta T| = \frac{3\hbar|\tau_{x0}|T}{\pi S(S+1)N_d(J_{sd}\rho)^2F(T)}. \tag{23}$$

To illustrate the application of this formula, consider the lithography scale of a memory element. We use the simplest macrospin equation for dynamics of a uniaxial free magnet having thickness w_{fm}, as before.[3] The threshold condition for switching without thermal activation over the energy barrier is $\hbar\tau_{x0} = \pm 2\alpha_G w_{fm} K_u$, where α_G is Gilbert damping and K_u is uniaxial anisotropy. To ensure static thermal memory stability assume $K_u v \cong 50 k_B T$ where $v = d^2 w_{fm}$ is the volume of the free magnet. Combining these relations yields the formula $|\hbar\tau_{x0}| = 100\alpha_G d^{-2} k_B T$. Substitution into Eq. (23) yields

$$|\delta T| = \frac{300\alpha_G k_B T^2}{\pi S(S+1)d^2N_d(J_{sd}\rho)^2F(T)}. \tag{24}$$

Assume, in addition to our previous parameter values, the lithography linewidth $d=30$ nm, $\alpha_G=0.02$, $F=10$ meV, and $T=300$ K. We find from Eq. (24) that a temperature differential as low as $|\delta T| \approx 10$ K at each interface may be sufficient to cause a thermagnonic switch.

VIII. PERPENDICULAR TORQUE

Note first that the y component of Eq. (6), in view of Eq. (8), has the lowest-order solution

$$\tau_y = \lambda\Sigma_0\sigma \sin\theta. \tag{25}$$

In the absence of the optional electric insulator shown in Fig. 1(a), nothing restrains the spin accumulation represented by σ from dispersing in the normal-metal thermal bath located at the right-hand extremity of this figure. So, in our ballistic model, we set $\nu_s \to \infty$ in Eq. (6) to find that σ must essentially vanish. Then, according to Eq. (25) $\tau_y = 0$.

However, the presence of an insulator (e.g., a 1-nm-thick MgO tunnel barrier) adjoining the free magnet as indicated in Fig. 1(a) will confine σ to the conduction electrons of the composite including the monolayer, normal metal, and free magnet. The coefficient ν_s is now finite and depends on the electron structure of this composite. In our ballistic limit, the z component of Eq. (6) now has the solution $\sigma = \nu_{ds}\delta\Sigma\cos\theta/\nu_s$. It is convenient to express the perpendicular torque component $\hbar\tau_y$ proportionally to $\hbar\tau_{x0}$. With the insulator present, elimination of $\nu_{ds}\delta\Sigma$ from the latter equation with Eq. (9) yields the normal-metal spin polarization

$$\sigma = \tau_{x0}\cos\theta/\nu_s. \tag{26}$$

After substitution of this equation into Eq. (25), one finds $\hbar\tau_y = -K_y \sin 2\theta$ where $K_y \sin^2\theta$ is the density of equivalent uniaxial surface magnetic anisotropy energy

$$K_y = \frac{-\lambda\hbar\Sigma_0\tau_{x0}}{2\nu_s}, \tag{27}$$

where $\Sigma_0 \equiv \chi_d F$ and χ_d is defined by Eq. (3). Thus the magnonic torque component $\hbar\tau_y$ simulates a uniaxial magnetic anisotropy whose axis is parallel to **F** and the ferrite moment $\mathbf{S}_{frt}$. Its magnitude depends on the parameters λ and ν_s which depend in part on electron structure of the free magnet and whose evaluation lies beyond the scope of the present communication.

The signs of τ_{x0} and K_y depend on the direction of heat flow. If heat flows from the ferrite toward the free magnet as in Fig. 1 ($\delta T > 0$), then $\tau_{x0} < 0$. If $\mathbf{S}_{frt}$ is parallel to an easy axis of total magnetic anisotropy for the free magnet, the torque component $\hbar\tau_x$ causes $\mathbf{S}_{fm}$ to precess and gradually tend to align with $-\mathbf{S}_{frt}$. Also, $K_y > 0$, making $\mathbf{S}_{frt}$ an easy axis for thermally induced effective anisotropy. Conversely, heat flow from the free magnet toward the ferrite would make $\tau_{x0} > 0$, tending to align $\mathbf{S}_{fm}$ with $\mathbf{S}_{frt}$. Also, $K_y < 0$, tending to make $\pm\mathbf{S}_{frt}$ an effective hard axis.

Finally, absence of the optional insulator shown in Fig. 1(a) has negligible effect on τ_x. However, τ_y now vanishes because the spin accumulation would not be constrained within a finite region and $\sigma = 0$ holds instead of the expression (26). Additional study involving the nature of the free magnet is needed to provide an estimate of the thermally induced effective magnetic anisotropy in the presence of the optional insulator.

IX. SUMMARY AND DISCUSSION

The quantum-yield parameter $\varepsilon(\geq 0)$ introduced by Eq. (1) is useful for comparing the effectiveness of thermal- and current-driven mechanisms of STT. We found above that for

the thermagnonic mechanism pertaining to Fig. 1(a), the in-plane torque is proportional to heat power VI times the sine of the angle θ between the two moments involved. Therefore, it takes the form

$$\Gamma_{\mathrm{tmg}} = \pm (\hbar/e)\varepsilon|I|(\mathbf{m}_{\mathrm{ref}} \times \mathbf{m}_{\mathrm{fm}}) \times \mathbf{m}_{\mathrm{fm}}. \tag{28}$$

Here, ε is a dimensionless device characteristic proportional to V, $\mathbf{m}_{\mathrm{fm}}$ is the unit vector moment of the free magnet, $\mathbf{m}_{\mathrm{ref}}$ is the unit moment of the static reference magnet, and $I=Q/V$ where V is the voltage that creates the heat flow Q. The $\pm$ sign varies with the direction of heat flow through the heterostructure shown in Fig. 1(a). A simple determination of this sign is given below.

In the case of an MTJ, the torque varies differently, in proportion to $V_{\mathrm{bar}}(\mathbf{m}_{\mathrm{ref}} \times \mathbf{m}_{\mathrm{fm}}) \times \mathbf{m}_{\mathrm{fm}}$,[21,22,44] and its sign varies with the sign of V_{bar}, the voltage across the barrier. In spite of these differences, direct comparison is possible because, in both cases, the in-plane torque for $\theta=\pi/2$ may be written $\Gamma_{\pi/2}=\pm(\hbar/e)\varepsilon|I|$. However, in the case of an MTJ, the yield $\varepsilon=\varepsilon_{\mathrm{mtj}}(\leq 1/2)$ is constant.

This communication began with the observation that the thermal magnons of a heated ferromagnet constitute a highly dense reservoir of mobile polarized spin. If all of this spin were available for transport to another, free ferromagnet, the quantum yield $\varepsilon_{\mathrm{htc}}$ of conveyed spin momentum per electron charge spent in Joule heating with applied voltage V would be of the order $e|V|/k_{\mathrm{B}}T$ which, per applied volt at $T=300$ K, is almost two orders of magnitude greater than the 1/2 maximum provided by conventional current-driven spin transfer using a MTJ.

More realistically, the interfacial dominance of thermal resistance in a very thin ferrite film implies that the transition $\Delta m_j=\pm 1$ in the magnetic energy $-Fm_j(m_j=-S,-S+1,\ldots,S)$ of the jth interfacial atomic moment determines the inherent quantum yield. This inherent yield amounts to $\varepsilon_{\mathrm{inh}}=|V|/F$. Since inferences from measured ferrite properties shown in Tables I and II indicate $F\approx 10$ to 20 meV, the inherent yield again approaches $\approx 10^2$ times that of an MTJ. The essential insight is that each "packet" $e|V|$ of Joule heat provided by the passage of one electron through the heater is capable of $e|V|/F$ spin transitions of amount $\Delta m_j=\pm 1$, each involving one $\hbar$ of spin momentum. Counterintuitively, the *smaller* the amount of energy F that is transferred, the *greater* is this inherent quantum yield $\varepsilon_{\mathrm{inh}}$ of transferred torque.

Parenthetically, one may observe that, within the ferrite, magnons transport both energy and spin momentum. Therefore the flows of heat and spin component are tightly bound together. But after a magnon annihilates at an interface with a normal metal, its lost energy contributes heat in the form of conduction-electron kinetic energy which, in the metal is not bound to the spin accumulation. The energy of spin accumulation is of higher order compared with that of the heat contained in kinetic energy of conduction electrons. Thus heat flow through the thickness of the spacer is essentially divorced from the spin flow.

Interesting in this connection is the fact that spin accumulation σ is not per se essential to in-plane thermagnonic spin transfer; only its time-derivative matters. Indeed, in our model σ vanishes in the absence of the "optional insulator" shown in Fig. 1(a); but not if this insulator is present. Yet, the in-plane torque differs negligibly. This circumstance differs from previous work[18] in which spin accumulation within the metal appears to drive the creation of magnons in the ferrite. This difference is attributable to our neglect of electron scattering within a very thin metallic spacer but not at its interfaces.

Alas, in practice the inherent yield $\varepsilon_{\mathrm{inh}}=|V|/F$ mentioned above is unavailable if phonons or conduction electrons, instead of magnons, carry too much of the heat flowing through the polarizing ferromagnet. Specifying a ferrite or other ferromagnetic insulator for the magnon source eliminates this threat from conduction electrons. But the effect of phonons may remain significant. Experimental data for the relevant Kapitza interfacial conductance G_{Kap} across a metal/ferrite interface is not available. The section "Estimates" (Sec. VI) above assumes low and high values of G_{Kap} measured for certain nonmagnetic compositions. It gives the predictions for $\varepsilon_{\mathrm{us}}/V$ from our theory plotted in Fig. 3 (for 100 ferrite texture) and 5 (for 110 ferrite texture) for three spinel-ferrite-film compositions. Some of the F values expected for interfacial magnetic ions Mn^{1+} and Fe^{2+} in Tables I and II are indicated in these plots. The positive slopes of these plots illustrate the fact that the Kapitza consideration replaces the inverse dependence of inherent quantum yield on F by a more credible, nearly proportional, dependence of useful yield.

The Curie-law condition, $F \ll 25$ meV at $T=300$ K, assumed in our analysis, is poorly satisfied by the values in Table I and II. Nonetheless, the plots in Figs. 3 and 4 indicate that even values of F small enough to satisfy the Curie-law limitation make possible an order-of-magnitude improvement, for $|V|\approx 1$ volt, of quantum yield over the existing $\varepsilon_{\mathrm{mtj}}\leq 1/2$ limitation of MTJs.

A rigorous qualitative argument gives directly the sign of the in-plane component of magnonic spin-transfer torque. Consider the case that heat flows from the ferrite toward the free magnet as in Fig. 1(a). Magnons bearing -1 spin component along the ferrite moment axis $S_{\mathrm{frt},\zeta}$ carry heat in the ferrite and, by our model, annihilate at the ferrite/spacer interface. By the law of continuity for macroscopic spin component, the ζ component of spin momentum transferred to the free magnet must also be negative. It follows that the free-magnet rate $d\mathbf{S}_{\mathrm{fm},\zeta}/dt$ and therefore the coefficient τ_{x0} must also be negative. [see Fig. 1(b)] Reversing the direction of heat flow changes these signs. However, reversing the sign of V in a Joule-effect heater will not change them.

The present theory indicates some key requirements for high useful yield of thermagnonic spin transfer. One is the provision of an interfacial magnetic layer with sufficiently large ferromagnetic ($F>0$) exchange coupling to the ferrite moment, as well as to the conduction electrons of the spacer metal with either sign of J_{sd}. Another is to ensure that the interfacial heat flow between the spacer and the phonon channel (and conduction-electron channel, if present) in the ferrite is sufficiently weak. Although the present theory treats explicitly a single paramagnetic monolayer, deposition of more than one layer of metallic magnetic atoms between the ferrite and spacer may also prove to be effective.

Applications of spin-transfer torque that may take advantage of a greater quantum yield include oscillators and MRAM. In a current-driven oscillator using an MTJ,[7] vortex formation in the free magnet favored by the magnetic field created by the electric current is one factor that may limit the size of the device. Replacement of electric current by flow of externally supplied heat to drive magnonic spin transfer may diminish this mechanism of vortex formation; it may permit an increase in the lithography scale and therefore the output voltage of such an oscillator. The greater torque per unit current available also implies the possibility of greater oscillation frequency if an appropriate free-magnet composition is selected.

The sign of the in-plane torque due to thermagnonic spin transfer varies with the direction of heat flow through the multilayer but not with the sign of any exciting electric current. Considerable ingenuity will be needed to overcome this disadvantage in potential applications to MRAM and disk storage. Compensating for this disadvantage is the opportunity for some combination of greater speed, greater density, and improved avoidance of errors due to thermal fluctuations.

Further theoretical work on thermally driven STT is needed. More study of the spin-pumping mechanism for spin coupling between ferrite and normal metal,[30] a possible alternative to the *sd* mechanism treated here, should establish the quantum yield expected. The fact that the expected magnitude of the spin-Seebeck effect using the ferrite YIG ($Y_3Fe_5O_{12}$) agrees with experiment[12] should encourage such an investigation.

ACKNOWLEDGMENTS

I thank Daniel Worledge for helpful comments on a previous draft of this paper. I also thank him, Jonathan Sun, Janusz Nowak, David Abraham, Guohan Hu, and Niladri Mojumder for useful discussions.

*slnczwsk@yahoo.com

[1] J. C. Slonczewski, Phys. Rev. B **39**, 6995 (1989).
[2] L. Berger, Phys. Rev. B **54**, 9353 (1996).
[3] J. C. Slonczewski, J. Magn. Magn. Mater. **159**, L1 (1996).
[4] J. A. Katine, F. J. Albert, R. A. Buhrman, E. B. Myers, and D. C. Ralph, Phys. Rev. Lett. **84**, 3149 (2000).
[5] S. Kiselev, J. C. Sankey, I. N. Krivorotov, N. C. Emley, R. J. Schoelkopf, R. A. Buhrman, and D. C. Ralph, Nature (London) **425**, 380 (2003).
[6] M. Hosomi, H. Yamagishi, T. Yamamoto, K. Bessho, Y. Higo, K. Yamane, H. Yamada, M. Shoji, H. Hachino, C. Fukumoto, H. Nagao, and H. Kano, Tech. Dig. - Int. Electron Devices Meet. **2005**, 459.
[7] A. M. Deac, A. Fukushima, H. Kubota, H. Maehara, Y. Suzuki, S. Yuasa, Y. Nagamine, K. Tsunekawa, D. D. Djayaprawira, and N. Watanabe, Nat. Phys. **4**, 803 (2008).
[8] T. Kimura, Y. Otani, and J. Hamrle, Phys. Rev. Lett. **96**, 037201 (2006).
[9] T. Yang, T. Kimura, and Y. Otani, Nat. Phys. **4**, 851 (2008).
[10] B. Heinrich, Y. Tserkovnyak, G. Woltersdorf, A. Brataas, R. Urban, and G. E. W. Bauer, Phys. Rev. Lett. **90**, 187601 (2003).
[11] Y. Tserkovnyak, A. Brataas, and G. E. W. Bauer, Phys. Rev. Lett. **88**, 117601 (2002).
[12] K. Uchida, S. Takahashi, K. Harii, J. Ieda, W. Koshibae, K. Ando, S. Maekawa, and E. Saitoh, Nature (London) **455**, 778 (2008); Solid State Commun. **150**, 524 (2010).
[13] K. Uchida, S. Takahashi, J. Ieda, K. Harii, K. Ikeda, W. Koshibae, S. Maekawa, and E. Saitoh, J. Appl. Phys. **105**, 07C908 (2009).
[14] M. Hatami, G. E. W. Bauer, Q. F. Zhang, and P. J. Kelly, Phys. Rev. B **79**, 174426 (2009).
[15] M. Hatami, G. E. W. Bauer, Q. Zhang, and P. J. Kelly, Phys. Rev. Lett. **99**, 066603 (2007).
[16] H. Yu, S. Granville, D. P. Yu, and J. P. Ansermet, Phys. Rev. Lett. **104**, 146601 (2010).
[17] Y. Kajiwara, K. Harii, S. Takahashi, J. Ohe, K. Uchida, M. Mizuguchi, H. Umezawa, H. Kawai, K. Ando, K. Takanashi, S. Maekawa, and E. Saitoh, Nature (London) **464**, 262 (2010).
[18] S. Takahashi, E. Saitoh, and S. Maekawa, J. Phys.: Conf. Ser. **200**, 062030 (2010).
[19] *Spin Caloritronics*, edited by G. E. W. Bauer, A. H. MacDonald, and S. Maekawa, Special issue of Solid State Commun. **150**, 459–552 (2010).
[20] I. L. Prejbeanu, M. Kerekes, R. C. Sousa, H. Sibuet, O. Redon, B. Dieny, and J. P. Nozières, J. Phys.: Condens. Matter **19**, 165218 (2007).
[21] H. Kubota, A. Fukushima, K. Yakushiji, T. Nagahama, S. Yuasa, K. Ando, H. Maehara, Y. Nagamine, K. Tsunekawa, D. D. Djayaprawira, N. Watanabe, and Y. Suzuki, Nat. Phys. **4**, 37 (2008).
[22] J. C. Sankey, Y. T. Cui, J. Z. Sun, J. C. Slonczewski, R. A. Buhrman, and D. C. Ralph, Nat. Phys. **4**, 67 (2008).
[23] Eq. (1.51) in L. R. Walker, in *Magnetism*, edited by G. T. Rado and H. Suhl (Academic Press, New York, London, 1963), Vol. I, Chap. 8.
[24] G. F. Dionne, *Magnetic Oxides* (Springer, New York, 2009).
[25] H. Hasegawa, Prog. Theor. Phys. **21**, 483 (1959).
[26] T. Sasada and H. Hasegawa, Prog. Theor. Phys. **45**, 1072 (1971).
[27] D. C. Langreth and J. W. Wilkins, Phys. Rev. B **6**, 3189 (1972); J. Sweer, D. C. Langreth, and J. W. Wilkins, *ibid.* **13**, 192 (1976).
[28] See Eq. (4.1) in H. Hasegawa (Ref. 25), or Eq. (1.7) in Sweer *et al.* (Ref. 27), and related formulas.
[29] J. Korringa, Physica (Amsterdam) **16**, 601 (1950).
[30] J. Xiao, G. E. W. Bauer, K. Uchida, E. Saitoh, and S. Maekawa, Phys. Rev. B **81**, 214418 (2010).
[31] V. S. Stepanyuk, L. Niebergall, R. C. Longo, W. Hergert, and P. Bruno, Phys. Rev. B **70**, 075414 (2004).
[32] D. M. Edwards, J. Mathon, R. B. Muniz, and M. S. Phan, Phys. Rev. Lett. **67**, 1476 (1991).
[33] K. Xia, P. J. Kelly, G. E. W. Bauer, A. Brataas, and I. Turek, Phys. Rev. B **65**, 220401 (2002).

[34] M. D. Stiles and A. Zangwill, Phys. Rev. B **66**, 014407 (2002).
[35] M. Zwierzycki, Y. Tserkovnyak, P. J. Kelly, A. Brataas, and G. E. W. Bauer, Phys. Rev. B **71**, 064420 (2005).
[36] R. J. Stoner and H. J. Maris, Phys. Rev. B **48**, 16373 (1993).
[37] G. D. Mahan, Phys. Rev. B **79**, 075408 (2009).
[38] J. J. Sakurai, *Modern Quantum Mechanics* (Benjamin, Menlo Park, CA, 1985), Sec. 5.6.
[39] W. H. Lien and N. E. Phillips, Phys. Rev. **133**, A1370 (1964).
[40] C. M. Hurd, J. Phys. Chem. Solids **30**, 539 (1969).
[41] D. A. Smith and G. B. Smith, Phys. Rev. B **4**, 191 (1971).
[42] J. Smit and H. P. J. Wijn, *Ferrites* (Wiley, New York, 1959).
[43] Chapter 4.3.1 of Ref. 24.
[44] J. C. Slonczewski and J. Z. Sun, J. Magn. Magn. Mater. **310**, 169 (2007).